

# Transmission area and two-photon correlated imaging

Yanfeng Bai, Shensheng Han, and Honglin Liu

*Key Laboratory for Quantum Optics and Center for Cold Atom Physics,*

*Shanghai Institute of Optics and Fine Mechanics,*

*Chinese Academy of Sciences, Shanghai 201800, China*

(Dated: August 6, 2018)

## Abstract

The relationship between transmission area of an object imaged and the visibility of its image is investigated in a lensless system. We show that the changes of the visibility are quite different when the transmission area is varied by different manners. An increase of the transmission by adding the slit number leads to a decrease of the visibility. While, the change is adverse when the slit width is widened for a given distance between two slits.

PACS numbers: 42.50.Dv, 42.50.Ar

arXiv:quant-ph/0611041v1 3 Nov 2006

The topic of two-photon correlated imaging has attracted much attention in recent years[1, 2, 3, 4, 5, 6]. The theory and experiment of ghost imaging with two-photon quantum entanglement were firstly demonstrated in mid-1990s[2, 3]. A fourth-order correlation function in the  $\{\mathbf{r}\}$  space is developed and applied to double-slit experiments with spontaneous down-conversion light by Barbosa[7]. Using the coupling between polarization entanglement and the entanglement for the transverse degrees of freedom, Caetano *et al.* demonstrated both theoretically and experimentally the manipulation of quantum entangled images[8]. The role of entanglement in two-photon imaging was discussed, Abouraddy *et al.* showed that entanglement is a prerequisite for achieving distributed quantum imaging[9]. While their work leads to some debate. Bennink *et al.* showed that coincidence imaging does not require entanglement, and provided an experimental demonstration using a classical source[10]. Using classical statistical optics, Cheng and Han studied a particular aspect of coincidence imaging with incoherent sources[11]. The first experimental demonstration of two-photon correlated imaging with true thermal light from a hollow cathode lamp was also reported[12].

Many objects imaged have been chosen since the theory of coincidence imaging was proposed. A double-slit was usually selected as an object in two-photon correlated imaging[6, 7, 10, 11, 12, 13, 14, 15, 16]. Cai and Zhu designed an optical system for implementing the second-order fractional Fourier transform for a single slit[17]. Eisebitt *et al.* demonstrated a versatile approach to perform lensless imaging of a sample consisting of a “H”, an “I”, and an open square at x-ray wavelength[18].

In this paper, we investigate the effects from transmission area of an object on the coincidence imaging with incoherent light source. Here transmission area is varied by two manners, increasing the slit number and slit width. We show that the effects are quite different under two conditions. Here the imaging system appropriate for correlated imaging is shown in Fig. 1. The light beam from the source  $S$  is incoherent, and divided into two beams by a beam splitter, they travel through a test and a reference arms, which are described by their impulse response functions  $h_1(x_1, u_1)$  and  $h_2(x_2, u_2)$ , respectively. The test arm usually includes an object to be imaged. Detector  $D_t$  is a pointlike detector,  $D_r$  is an array of pixel detector, which are used to record the intensity distribution of the photons at  $u_1$  and  $u_2$ , respectively.

The optical field in the source can be represented by  $E(x)$ . After propagating through

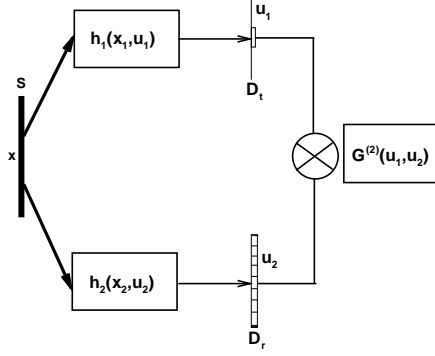


FIG. 1: Two-photon correlated imaging with incoherent light.

two different optical systems, the field has

$$E_i(u_i) = \int E(x)h_i(x, u_i)dx, \quad i = 1, 2. \quad (1)$$

The fourth-order correlation function at  $u_1$  and  $u_2$  may be recorded with the coincidence rate in the test and reference detectors

$$G^{(2)}(u_1, u_2) = \langle E(u_1)E(u_2)E^*(u_2)E^*(u_1) \rangle, \quad (2)$$

where  $E(u_i)$  ( $i = 1, 2$ ) is the optical field in the test (reference) detector. Substituting Eq. (1) into Eq. (2), we have

$$\begin{aligned} G^{(2)}(u_1, u_2) = & \int \int \int \int \langle E(x_1)E(x_2)E^*(x'_2)E^*(x'_1) \rangle \\ & \times h_1(x_1, u_1)h_2(x_2, u_2)h_2^*(x'_2, u_2) \\ & \times h_1^*(x'_1, u_1)dx_1dx_2dx'_2dx'_1, \end{aligned} \quad (3)$$

where  $\langle E(x_1)E(x_2)E^*(x'_2)E^*(x'_1) \rangle$  is the four-order correlation function at the light source, We represent it by  $G^{(2)}(x_1, x_2, x'_2, x'_1)$  in the following in order to outline the parallelism with the formalism in Eq. (2).

In many cases, the fluctuation of a classical light field can be characterized by a Gaussian field statistics with zero mean[19], one obtains

$$\begin{aligned}
G^{(2)}(x_1, x_2, x'_2, x'_1) &= G^{(1)}(x_1, x'_1)G^{(1)}(x_2, x'_2) \\
&+ G^{(1)}(x_1, x'_2)G^{(1)}(x_2, x'_1),
\end{aligned} \tag{4}$$

where  $G^{(1)}(x_i, x_j)$  is the second-order correlation function of the fluctuating source field, and arbitrary order correlation function is thus expressed via the second-order correlation function

$$G^{(1)}(x_i, x_j) = \langle E(x_i)E^*(x_j) \rangle, \tag{5}$$

along with the relation  $G^{(1)}(x_i, x_j) = [G^{(1)}(x_j, x_i)]^*$ . By using Eqs. (4) and (5), we can simplify Eq. (3) as

$$\begin{aligned}
G^{(2)}(u_1, u_2) &= \int \int \langle E(x_1)E^*(x'_1) \rangle h_1(x_1, u_1)h_1^*(x'_1, u_1) dx_1 dx'_1 \\
&\times \int \int \langle E(x_2)E^*(x'_2) \rangle h_2(x_2, u_2)h_2^*(x'_2, u_2) dx_2 dx'_2 \\
&+ \int \int \langle E(x_1)E^*(x'_2) \rangle h_1(x_1, u_1)h_2^*(x'_2, u_2) dx_1 dx'_2 \\
&\times \int \int \langle E(x_2)E^*(x'_1) \rangle h_2(x_2, u_2)h_1^*(x'_1, u_1) dx_2 dx'_1 \\
&= \langle I(u_1) \rangle \langle I(u_2) \rangle + \left| \int \int \langle E(x_1)E^*(x'_2) \rangle h_1(x_1, u_1)h_1^*(x'_2, u_2) dx_1 dx'_2 \right|^2 \\
&= \langle I(u_1) \rangle \langle I(u_2) \rangle + \Delta G^{(2)}(u_1, u_2).
\end{aligned} \tag{6}$$

The information of the object imaged is extracted by measuring the spatial correlation function of the intensities  $\langle I(u_1)I(u_2) \rangle$ . By subtracting the background term  $\langle I(u_1) \rangle \langle I(u_2) \rangle$ , we can obtain the correlation function of intensity fluctuations, all information about the object is contained in it

$$\Delta G^{(2)}(u_1, u_2) = \langle I(u_1)I(u_2) \rangle - \langle I(u_1) \rangle \langle I(u_2) \rangle, \tag{7}$$

Theoretically the visibility which is our concern in this paper is defined as

$$\begin{aligned}
V &= \frac{\Delta G^{(2)}(u_1, u_2)_{max}}{\langle I(u_1)I(u_2) \rangle_{max}} \\
&= \frac{\Delta G^{(2)}(u_1, u_2)_{max}}{\left[ \langle I(u_1) \rangle \langle I(u_2) \rangle + \Delta G^{(2)}(u_1, u_2) \right]_{max}}.
\end{aligned} \tag{8}$$

It has been known that, from the discussion in Ref. [20],  $\Delta G^{(2)} \leq \langle I(u_1) \rangle \langle I(u_2) \rangle$  in the thermal case, so the visibility is never above 0.5. In the following, we will investigate the effects from the transmission area of an object on the visibility.

For incoherent light, we assume that its intensity distribution is of the Gaussian type. Then the two-order correlation function for completely incoherent light source can be written as

$$\langle E_s(x_1)E_s^*(x_2) \rangle = G_0 \exp\left(-\frac{x_1^2 + x_2^2}{4a^2}\right) \delta(x_1 - x_2), \quad (9)$$

where  $G_0$  is a normalized constant,  $a$  is the transverse size of the source.

In the test arm, an object (transmission function  $t(x')$ ) is located at a distance  $z_1$  from the source  $S$  and a distance  $z_2$  from detector  $D_t$ . Thus the impulse response function can be expressed as

$$\begin{aligned} h_1(x_1, u_1) = & \int \frac{e^{-ikz_1}}{i\lambda z_1} \exp\left[\frac{-i\pi}{\lambda z_1}(x' - x_1)^2\right] t(x') \\ & \times \frac{e^{-ikz_2}}{i\lambda z_2} \exp\left[\frac{-i\pi}{\lambda z_2}(u_1 - x')^2\right] dx'. \end{aligned} \quad (10)$$

The reference arm contains nothing but free-space propagation from  $S$  to  $D_r$ . Thus the corresponding impulse response function under the paraxial approximation is

$$h_2(x_2, u_2) = \frac{e^{-ikz}}{i\lambda z} \exp\left[\frac{-i\pi}{\lambda z}(u_2 - x_2)^2\right], \quad (11)$$

we know that, from the conclusion in Ref. [11], such a coincidence imaging system realizes the function of Fourier transform imaging under the condition of a large, uniform, fully incoherent light source. Here, we take a double slit with slit width  $\omega = 0.075\text{mm}$  and the distance between two slits  $d = 0.15\text{mm}$  as the object imaged. The transverse size of the source  $a = 1\text{mm}$ , other parameters are chosen as  $\lambda = 532\text{nm}$ ,  $z = 175\text{mm}$ ,  $z_1 = 75\text{mm}$ , and  $z_2 = z - z_1$ .

Substituting Eqs. (9)-(11) into Eq. (6), we can get the normalized conditional coincidence rate, the numerical simulation results will be analyzed. Here, we provide two methods to change the transmission area of the object imaged. Firstly, we increase the slit number. The images are given in Fig. 2(a). From our simulations it clearly emerges that, under the given parameters, the quality of the Fourier-transform imaging gets better, whereas the visibility

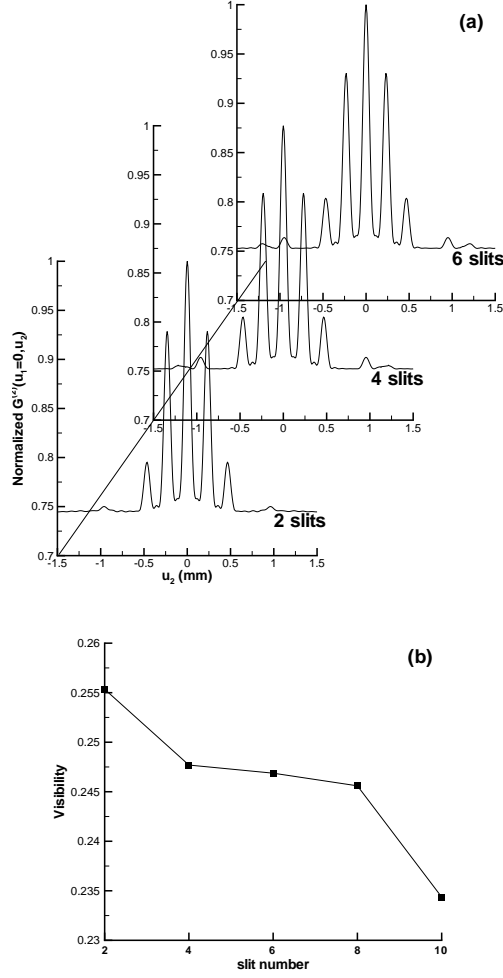


FIG. 2: (a) The normalized conditional coincidence rate  $G^{(2)}(0, u_2)$  versus  $u_2$  with incoherent light source for different slit number. (b) Dependence of the corresponding visibility on the slit number  $n$ .

is decreased with an increase of slit number, i.e., the transmission area. The corresponding experiment results have been implemented in a  $f$ - $2f$  system[21].

To make our results more general, in Fig. 2(b), we give the visibility under different slit number  $n$ . Here, we only depict the dots for finite slits because the ghost imaging will be distorted when  $n$  is much large. It is clear that the visibility will decrease with the increase of the slit number.

Secondly, we vary the transmission area by increasing the ratio of the slit width to slit distance,  $\omega/d$ , for a given slit distance  $d = 0.15\text{mm}$ , the results are depicted in Fig. 3(a). An increase of the slit width leads to an increase of the image visibility, while the image

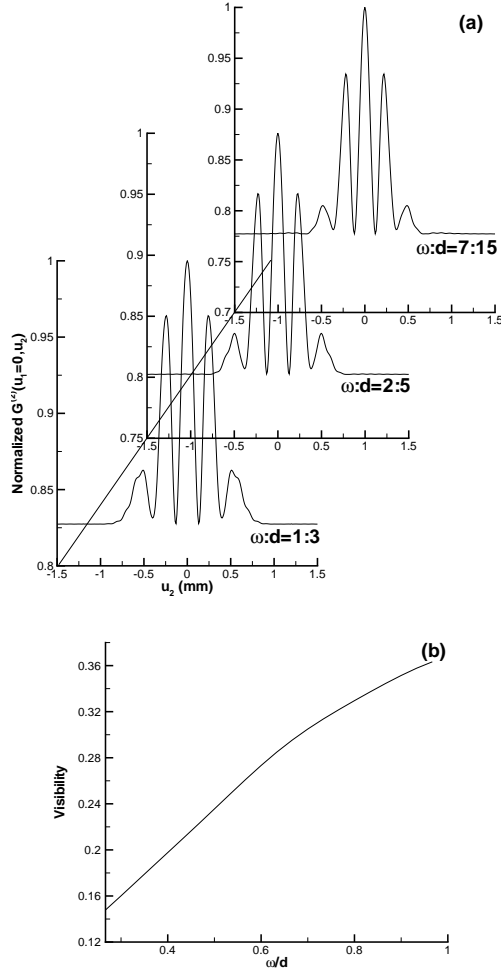


FIG. 3: (a) The normalized  $G^{(2)}(0, u_2)$  as the function of  $u_2$  for different ratios of the slit width to slit distance. (b) The corresponding visibility versus  $\omega/d$ .

quality gets worse during this process. It should be noticed, by comparing with the curves in Fig. 2(a), the change of the visibility by widening the slits is much bigger than that by increasing the slit number.

In Fig. 3(b), we show the dependence of the visibility on the normalized slit width  $\omega/d$ . The images are distorted when  $\omega$  is much smaller or close to  $d$ , so the dots should be subtracted. Here we obtain a curve of the visibility completely different from that in Fig. 2(b). The increase of the slit width, i.e., the transmission area, makes the visibility enhance.

From the results in Figs. 2(b) and 3(b), the variation ranges of the visibility we obtain coincide with the prediction value in Ref. [20]. While the visibility is so poor that the images can not be observed during practical experiment implementation, so we usually retrieve the

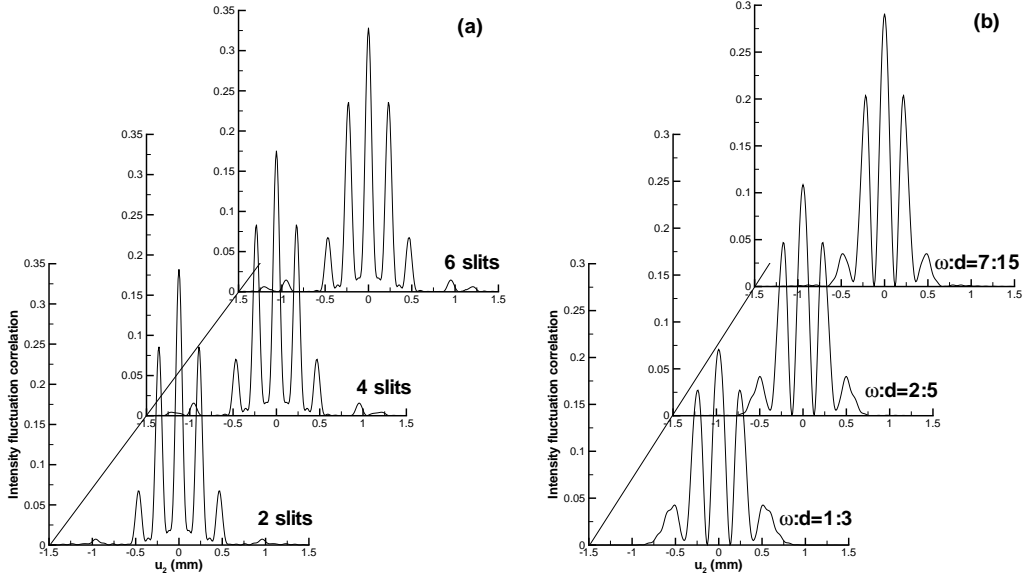


FIG. 4: Normalized  $\Delta G^{(2)}(0, u_2)$  vs the reference detector position for an object with different transmission. (a) Intensity fluctuation correlations for different slit number. (b) The curves for different slit width.

desired information, i.e., the intensity fluctuation correlation by subtracting the background, as shown in Fig. 4. Comparing the curves which are normalized by  $\langle I(u_1) \rangle \langle I(u_2) \rangle$ , we can draw the same conclusion that both decreasing the slit number and increasing the slit width make the visibility enhance.

With the technology development of correlated imaging, one is not satisfied with the Fourier-transform images only for simple objects, some complex objects are being considered. Here there are still many questions unresolved, such as what limits the visibility for complex object. Based on the above discussions, we can enhance the visibility of correlated imaging by choosing proper slit number and slit width when other parameters are given. Which can be helpful in the realistic experiments of two-photon correlated imaging.

In conclusion, we give the theoretical analysis of the relationship between the transmission area and the visibility in a correlated imaging with incoherent light. Though the transmission area can be varied by changing the slit number or width, they have different effects on the visibility. The visibility gets worse with an increase of the slit number, whereas an increase of the slit width leads to an increase of the visibility.

The work was supported by the National Natural Science Foundation of China under

Grant No. 60477007, and the Shanghai Optical-Tech Special Project (grant 034119815).

---

- [1] P. H. S. Ribeiro, S. Padua, J. C. Machado da Silva, and G. A. Barbosa, *Phys. Rev. A* **49**, 4176 (1994).
- [2] A. V. Belinsky and D. N. Klyshko, *Sov. Phys. JETP* **78**, 259 (1994).
- [3] T. B. Pittman, Y. H. Shih, D. V. Strekalov, and A. V. Sergienko, *Phys. Rev. A* **53**, R3429 (1995).
- [4] D. V. Strekalov, A. V. Sergienko, D. N. Klyshko, and Y. H. Shih, *Phys. Rev. Lett.* **74**, 3600 (1995).
- [5] A. F. Abouraddy, B. E. Saleh, A. V. Sergienko, and M. C. Teich, *J. Opt. Soc. Am. B* **19**, 1174 (2002).
- [6] A. Gatti, E. Brambilla, and L. A. Lugiato, *Phys. Rev. Lett.* **83**, 1763 (1999); **90**, 133603 (2003).
- [7] G. A. Barbosa, *Phys. Rev. A* **54**, 4473 (1996).
- [8] D. P. caetano, P. H. Souto Ribeiro, J. T. C. Pardal, and A. Z. Khoury, *Phys. Rev. A* **68**, 023805 (2003).
- [9] A. F. Abouraddy, B. E. Saleh, A. V. Sergienko, and M. C. Teich, *Phys. Rev. Lett.* **87**, 123602 (2001).
- [10] R. S. Bennink, S. J. Bentley, and R. W. Boyd, *Phys. Rev. Lett.* **92**, 033601 (2004).
- [11] Jing Cheng and Shensheng Han, *Phys. Rev. Lett.* **92**, 093903 (2004).
- [12] Da Zhang, Yanhua Zhai, Ligan Wu, and Xihao Chen, *Opt. Lett.* **30**, 2354 (2005).
- [13] A. Gatti, E. Brambilla, M. Bache, and L. A. Lugiato, *Phys. Rev. A* **70**, 013802 (2004).
- [14] Sang-Kyung Choi, M. Vasilyev, and P. Kumar, *Phys. Rev. Lett.* **83**, 1938 (1999).
- [15] D. Magatti, F. Eerri, A. Gatti, M. Bache, E. Brambilla, and L. A. Lugiato, arXiv.org e-Print archive, arXiv. quant-ph/0408021, (2004).
- [16] Jing Cheng and Shensheng Han, *Chin. Phys. Lett.* **22**, 1676 (2005).
- [17] Yangjian Cai, and Shiyao Zhu, *Opt. Lett.* **30**, 388 (2005).
- [18] S. Eisebitt, M. Lorgen, and W. Eberhardt, *Appl. Phys. Lett.* **84**, 3373 (2004).
- [19] J. W. Goodman, *Statistical Optics* (Wiley, New York, 1985).
- [20] M. Bache, D. Magatti, F. Ferri, A. Gatti, E. Brambilla, and L. A. Lugiato, *Phys. Rev. A* **73**,

053802 (2006).

- [21] Honglin Liu, Jing Cheng, Yanfeng Bai, and Shensheng Han, arXiv.org e-Print archive, arXiv:quant-ph/0609146, (2006).